九州大学学術情報リポジトリ
Kyushu University Institutional Repository

Dispersion of passive pollutant within and above various urban canopies

Bezpalcová, Klára
Institute of Thermomechanics, Academy of Sciences, v.v.i.

Ohba, Masaaki
Department of Architecture, Tokyo Polytechnic University

https://hdl.handle.net/2324/13283

出版情報：COE Lecture Note. 14, pp.3-13, 2009-02-12. 九州大学大学院数理学研究院
バージョン：
権利関係：

Proceedings of the Czech-Japanese Seminar in Applied Mathematics 2008
Takachiho / University of Miyazaki, Miyazaki, Japan, September 1-7, 2008
pp. 3-13

DISPERSION OF PASSIVE POLLUTANT WITHIN AND ABOVE VARIOUS URBAN CANOPIES

KLÁRA BEZPALCOVÁ[1] AND MASAAKI OHBA[2]

Abstract.
Releases of harmful gaseous materials within the lower part of the atmospheric boundary layer are of high concern of the society in general. The understanding of short-range dispersion of air-borne substances within the urban canopy is crucial to predict spread of such pollutants. Mathematical modelling has to deal with many approximations or/and computer capacity limitations while solving such a complex task. Physical modelling is an alternative method that was used for investigation of the dispersion of a passive pollutant. The idealised urban canopies were created by regular cubes which were collocated at three different packing densities and two different patterns. The flow and concentration of the passive tracer released from the ground level source were measured simultaneously. Various single- as well as cross-statistics was derived. The terms describing purely advective and turbulent transport of the passive contaminant were measured by using a unique method. The comparison of those fluxes within 6 different arrangements of idealised urban canopies is shown and the importance of a proper determination of the turbulent fluxes at the edge of the plume and above the roof top level is emphasised.

Key words. Atmospheric Dispersion, Air Pollution, Wind Tunnel

AMS subject classifications. 86-05, 86A10, 76F25, 76F40

1. Introduction. Dispersion of pollutants in urban areas is still one of the most challenging tasks in environmental sciences. Complex processes like the dispersion of car exhaust in street canyons or the dispersion of accidental releases of harmful substances in built-up areas are not yet fully understood. For a better insight of the driving phenomena it is helpful to study flow and dispersion of pollutants within an idealised urban setting first.

The study of dispersion through large idealised arrays of building-like obstacles is an important method of obtaining a better understanding of dispersion through a real urban environment. Field and laboratory studies of idealised obstacle arrays are necessarily simplifications of the real complex urban environment. However, the idealised canopy can reproduce some of the real urban characteristics as building packing density or building arrangement. These types of geometries, nonetheless, should display some of the characteristics of the more complex, real-world configurations, and show some generally valid rules. We examined flow and passive tracer dispersion within 6 different configurations of the idealised urban area layout during our experiment. The objective of the presented paper is the analysis of the mean concentration field at the street level for different idealised urban canopy set-ups and showing the main mechanism of the pollutant transport within them. Such knowledge should play a significant role in design process of new urban structures or modification of already built-up areas to achieve better ventilation characteristics.

One of the first experiments dealing with an idealised urban canopy was conducted by MacDonald et al. [1], who compared the mean concentration characteristics within the idealised urban canopies with different packing densities. They did not find any

[1]Institute of Thermomechanics, Academy of Sciences, v.v.i., Prague, Czech Republic.
[2]Department of Architecture, Tokyo Polytechnic University, Atsugi, Japan.

significant differences between different packing densities and neither did Mavroidis [2] in his work. Cheng et al. [3] investigated the drag forces and momentum transport for two packing densities and aligned/staggered arrangement. They found significantly increased drag and momentum transport for the staggered arrays. Therefore, an enhanced vertical transport of passive contaminant could be expected.

The vertical ventilation of the toxic gaseous pollutant from the street level to the relatively unobstructed flow above the urban canopy is the main interest of our study. Simultaneous measurement of passive tracer concentration and vertical wind component with high temporal resolution is very unique and allows us to directly derive the advective and turbulent vertical transport terms WC and $w'c'$ from the equation of advection (see below, [4]). The magnitude of the terms depends on the character of flow in the given place and can vary significantly. There are not many papers concerning the concentration fluxes. Fackrell and Robins [5] examined these fluxes in unobstructed atmospheric boundary layer flow and found that turbulent and advective transports are of the same magnitude. The magnitude of the turbulent transport of passive contaminant was found significant due to the suppressing of the mean flow within the plant canopy (Meyers [6]).

2. Definitions. The advection equation for a scalar ψ, such as concentration of passive contaminant, far from the source of the scalar is expressed mathematically as:

$$\frac{\partial \psi}{\partial t} + \nabla \cdot (\psi \mathbf{u}) = 0, \tag{2.1}$$

where ∇ is the divergence operator and $\mathbf{u}$ is the velocity vector field. Any variable within the turbulent field can be divided to the temporally constant mean value (depicted by overbar) and fluctuating part (depicted by prime), which time average mean value is zero. Therefore we can rewrite the temporal mean equation of advection as:

$$\psi = \overline{\psi} + \psi' \Rightarrow \frac{\partial \overline{\psi}}{\partial t} + \nabla \cdot (\overline{\overline{\psi}\overline{\mathbf{u}}} + \overline{\psi' \mathbf{u}'}) = 0. \tag{2.2}$$

The second term on the left hand side of the equation 2.2 of advection has two parts. The first term is product of the mean values of velocity and concentration and it describes the purely advective changes in the scalar field. The second part is mean value of the product of the fluctuating parts and it describes a turbulent contribution to the changes in the scalar field. The magnitude of both parts is dependent on the character of flow in the given place and can vary significantly.

The ventilation of the toxic gaseous pollutant is the main interest of our study. If we look at the situation from the point of view of the street inhabitants and looking for the most suitable solution of a high pollutant concentration, the most preferable way of the ventilation of those pollutants is vertical. Vertical ventilation will transport pollutants to the relatively free stream above the urban canopy and there the pollutants concentration will be quickly reduced. Therefore we focused on the vertical component of the equation of passive contaminant advection:

$$\frac{\partial \overline{c}}{\partial t} + \frac{\partial}{\partial z}(\overline{CW} + \overline{c'w'}) = 0. \tag{2.3}$$

where W and w' is the mean and fluctuation part of vertical wind component, respectively, and C and c' is the mean and fluctuation part of concentration of passive contaminant. The first and second term in the brackets are called the advective and turbulent vertical flux of the passive pollutant, respectively.

(a) Urban canopy model C_25_A, spires and roughness elements.

(b) Split fiber probe and fast ionisation detector.

FIG. 3.1. *Urban canopy model and instrumentation.*

3. Experimental set-up. The experiment was carried out in the Boundary Layer Wind Tunnel at Wind Engineering Center of Tokyo Polytechnic University, Atsugi, Japan. The 14 m long facility provides test section equipped with turntable and the cross section of the tunnel measures 1.2 m in width and 1 m in height. Measuring instrumentations (see Fig.3.1(b)) were placed on a controlled positioning system, which allowed to move the probes in all 3 directions and to rotate the z-axis. Spires and roughness elements were used to develop model of the suburban atmospheric boundary layer in the scale 1:400.

The spires are two-dimensional structures placed at the very beginning of the development section of the wind tunnel (just behind the stilling chamber). The roughness elements had dimensions: 50mm (width), 50mm (length), 25mm (height). The roughness elements were placed in regular pattern. Spires and roughness elements together with one of the idealised urban area models are shown in Fig.3.1.

The researcher team of Wind Engineering Center of Tokyo Polytechnic University has developed new method for simultaneous measurement of velocity and concentration by the means of constant temperature thermo-anemometry (CTA) and flame ionisation detection (FID) of the tracer gas (Yoshie et al., [7]). This set-up allows to derive turbulent fluxes related to the momentum and concentration. The flow measurement was conducted using CTA with split-fibre probe and constant temperature adjustment module. The concentration measurements were performed by fast FID. The mounting of the instruments is shown in Fig.3.1. The analog signal from both instruments was first filtered by 200 Hz low-pass filter to reduce data noise and then converted by an A/D convertor. Data sampling rate was 1 kHz.

All of the idealised urban canopy set-ups consisted of identical sharp edged wooden cubes of side 70mm. They were arranged in the regular aligned or staggered arrays with different obstacle spacing. Obstacle spacing, L, is sometimes replaced by aspect ratio, which is defined as L/H, where H is average building height. There were always at least 7 rows of cubes in front of and 8 rows behind the source; each consisted at least of 7 cubes. The actual number varied according to the set-up. The arrangement parameters and set-up labelling is shown in Table 1. The scale of the model and of the modelled boundary layer was 1:400, i.e. the building height would

be equivalent to 28 m in the full scale.

The ground-level point source of the tracer gas ethylene (C_2H_4) was located in the wake of the cube at coordinates x = -5.43H, y = 0H, and z = 0H (coordinates and the origin are shown in Fig.5.1). The location was the same for all set-ups. Density of ethylene is 1.18 kg m^{-3} in standard atmospheric conditions and it can be considered as a passive tracer because its density is very close to standard air density (1.2 kg m^{-3}). The molecular diffusivity is negligible compared to the turbulent diffusivity.

The experimental conditions were carefully checked by series of measurements. The independence of dimensionless properties on the source emission rate Q and Building Reynolds number Re_B were found for experiments with $Q > 50$ cc/min and Re_B >12000 (i.e. $U_H > 6$ m/s), respectively. The characteristic experimental conditions were: $Q \approx 300$ cc/min (i.e. 18 l per hour) and $Re_B \approx 16000$ cc/min (i.e. $U_H \approx 8$ m/s).

TABLE 3.1
Experimental conditions.

Aspect ratio (L/H)	0.71	1	1.5
Packing density	34%	25%	16%
Aligned type	C_34_A	C_25_A	C_16_A
Staggered type	C_34_S	C_25_S	C_16_S

4. Modelled boundary layer. The logarithmic law describing mean wind vertical profile, $U(z)$, in the lower part of the atmospheric boundary layer can be mathematically written as:

$$U(z) = \frac{u_*}{\kappa} \ln \frac{z - d_0}{z_0}, \tag{4.1}$$

where u_* is friction velocity, κ=0.4 is von Karman constant, d_0 is displacement height, and z_0 is roughness length. Another way how to describe the mean wind vertical profile is the power law:

$$U(z) = U_{\text{ref}} \left(\frac{z}{z_{\text{ref}}} \right)^{\alpha}, \tag{4.2}$$

where U_{ref} is reference wind speed at reference height z_{ref} and α is power law exponent. More about the properties of the atmospheric boundary layer can be found in [8].

Measured mean wind speed vertical profile is shown in Fig.4.1(a). Logarithmic and power law profiles were applied to the measured profile with following parameters (in full scale): roughness length z_0=1m, displacement length d_0=3.2m, friction velocity u_*=0.44 m/s, and power law exponent α=0.25. These parameters correspond to those observed in atmospheric boundary layer above moderately rough terrain (see [9]). Also high order statistical moments were measured and compared to full scale data. Vertical profile of turbulence intensity compared to the empirical formula proposed by Snyder [9] and dimensionless power spectra compared with empirical formula proposed by Kaimal et al. [10] are shown in Fig.4.1(b) and 4.1(c), respectively. For more detailed description of the boundary layer see [11].

5. Mean concentration field. Since the experiments were conducted in the scale, we need to define dimensionless or normalized variables to obtain values, which

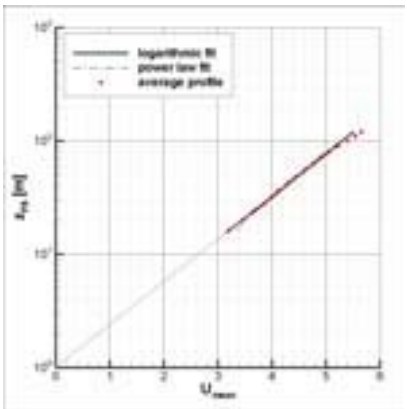

(a) Vertical profile of mean wind speed.

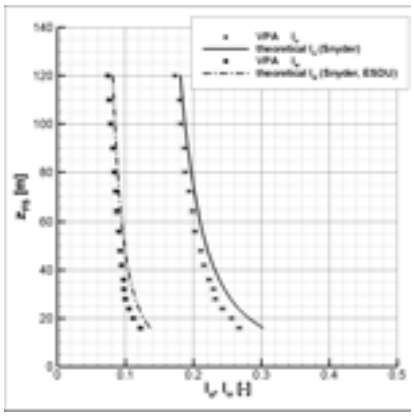

(b) Vertical profiles of turbulent intensity for u and w wind components.

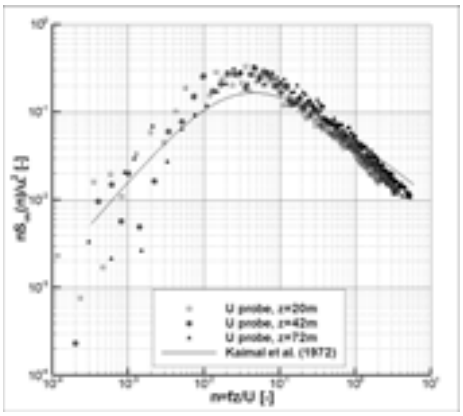

(c) Dimensionless power spectra for u wind component at 3 different heights.

FIG. 4.1. *Modelled boundary layer characteristics.*

can be compared with the other experiments or numerical simulations. All the coordinates are given as a ratio of the building height H. The non-dimensional concentration is defined according to equation:

$$c^* = \frac{c\,U_H\,H^2}{Q}, \tag{5.1}$$

where c is measured concentration, H=70mm is the building height, U_H is the average wind speed at 1.5 times building height (z=105mm, or 42 m in full scale when the model scale is 1:400), and Q is the source emission rate.

The mean concentration distribution of the passive tracer gas at the height of 0.29H for the different urban set-ups is shown in Fig.5.1. The figures have the same exponential concentration scale that ensures a clear insight to the plume structure

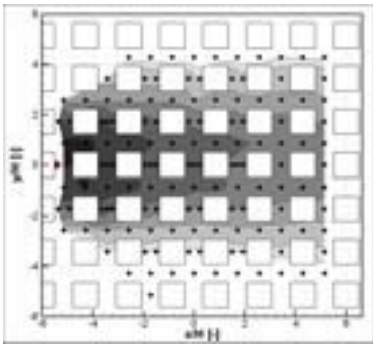

(a) Set-up C_34_A.

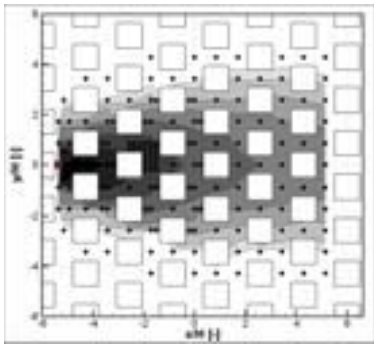

(b) Set-up C_34_S.

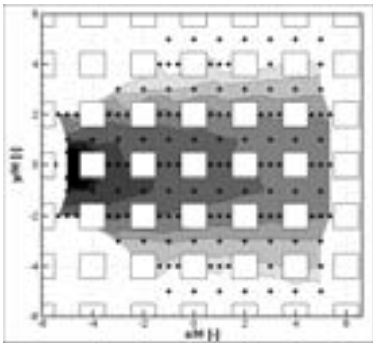

(c) Set-up C_25_A.

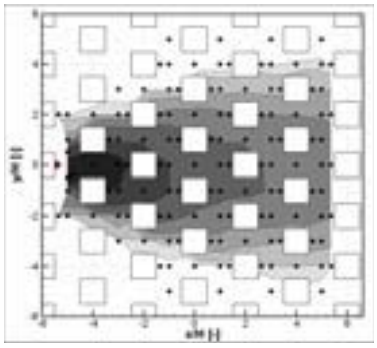

(d) Set-up C_25_S.

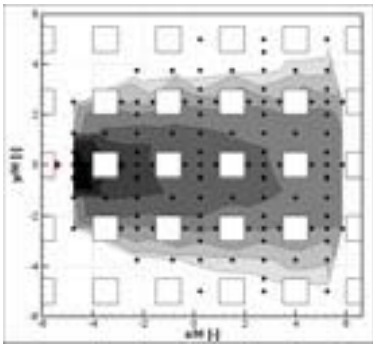

(e) Set-up C_16_A.

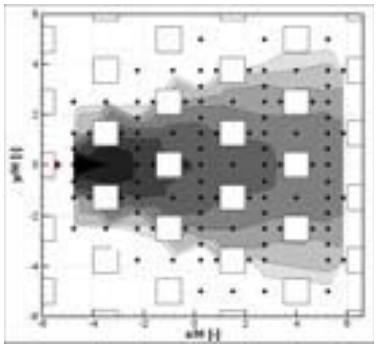

(f) Set-up C_16_S.

FIG. 5.1. *Mean dimensionless concentration c^* at height z=0.29H.*

at all positions as well as a direct comparison of the results for different set-ups. There were approximately 130 measurement points per set-up and they are depicted in Fig.5.1 by small black diamonds. An interpolation was used to create the contour plots.

The differences between plume shapes are evident. The wide spread of the tracer immediately after release, i.e. inside the street canyon where the point source was located, is distinctive for the aligned set-ups. In this case all the pollutant is kept in the range $y \in (-4; 4)$ independently on the packing densities. On the other hand, the initial spread is not so wide and the concentrations reach high values only behind the central cube and the surrounding street canyons for the staggered set-ups. The lateral spread continues downwind creating a triangle shape plume rather than rectangle shape as in the case of the aligned arrays. The less-packed set-ups showed slightly larger area, where the threshold was exceeded than denser packed set-ups considering the concentration thresholds given in Fig.5.1. The plume shape differs according to arrangement pattern. The plume is longer but thinner in the case of staggered arrays. We computed the area integral of the exceeding area for all set-ups and the thresholds depicted in Fig.5.1. The exceeding area for given threshold was always smaller in the case of staggered arrays than within the aligned set-ups. This means that the ground level area threatened by the toxic gas release is larger due to weaker vertical transport in the less dense and aligned set-ups.

The comparison with previous experiments (e.g. by MacDonald et al. [1] and Mavroidis [2]) is difficult because of the significant difference in the release conditions. In the other studies the tracer gas was emitted in front of the building array to the boundary layer free stream. Therefore a wide lateral spreading of the tracer close to the source was not observed. The difference in the plume shape for aligned/staggered set-ups was clearly shown in Fig.5.1 due to much better spatial resolution of the measurement points than the previous experiments had.

6. Vertical flux of passive contaminant. There are two main directions of passive contaminant transport, horizontal and vertical advection. Less dense and aligned set-ups allow higher wind speeds at the street level compared to denser and staggered set-ups. However, smaller concentration at lower elevations in the case of the denser set-ups is caused by the enhanced vertical transport of passive tracer. The vertical wind speed component and the concentration of passive tracer gas were measured simultaneously at one place to obtain the normalised vertical advective and turbulent fluxes $WC^*/U_H \cdot 100$ and $w'c^{*\prime}/U_H \cdot 100$, respectively. The example of the fluxes distribution within the C_25_S set-up is given in Fig.6.1. The turbulent, advective, and total vertical fluxes of the passive tracer are shown. Since the magnitude of the advective vertical flux is predominant in most of the field, Fig.6.1(c) was added to highlight the points where the turbulent transport contributes significantly. The symbols have the shading according to the total flux magnitude, shape of the symbol shows direction of the flux (diamonds upward, circles downwards), and the size is determined be the ratio of the turbulent flux within the total flux.

The turbulent flux contributes significantly to the total flux at the edges of the plume in both directions. The concentration signal is highly intermittent with very small mean values there. Therefore, the advective flux is also very small. Nonetheless, the nonzero turbulent vertical transport indicates that peak concentration values are significant and coincident with certain flow patterns. The upward vertical turbulent transport was found in the first and second street canyon behind the source, which reflects the coincidence of higher concentrations with stronger upward wind speed. In

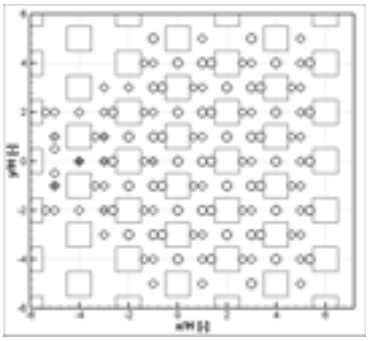

(a) Turbulent vertical transport $w'c'^*$.

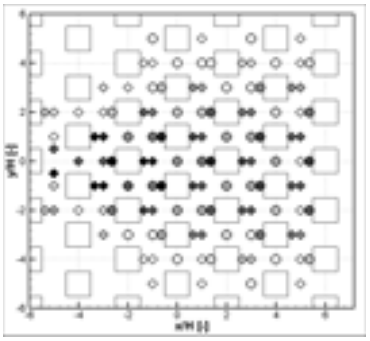

(b) Advective vertical transport WC.

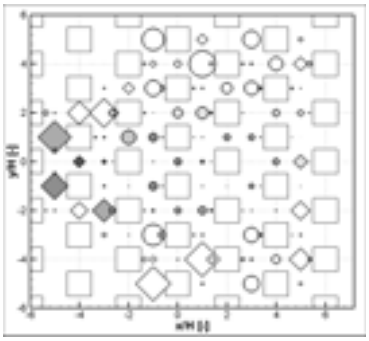

(c) Total transport $w'c'^* + WC$.

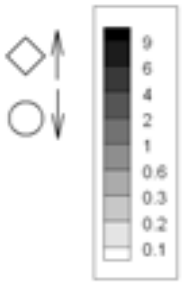

FIG. 6.1. *Normalised vertical transport at height 0.27H within the C_25_S set-up.*

contrary, mostly the downward vertical turbulent transport was found in the further positions. This illustrates the fact that after the initial upward vertical ventilation of the passive pollutant released from ground source the pollutant penetrates back to the canopy from the free stream in the further positions.

There is an obvious dependence of the vertical flux value on the position with respect to the cube layout. The vertical profiles of the advection and turbulent vertical transport, and Reynolds stress, $u'w'$, in the leeward and windward positions are shown in Fig.6.2. The measurement positions were located in the middle of the plume in the second street canyon behind the source of the passive tracer at coordinates x/H=-1.36, y/H=0 and x/H=-0.64, y/H=0 for the leeward and windward profiles, respectively. The space adjacent to the leeward and windward facades plays a crucial role in the vertical transport of the passive pollutants from the ground level. The mean vertical velocity is negative in the windward regions and positive in the leeward regions following the well-know street canyon vortex layout [12]. Therefore, the sign of the advective vertical transport is given. Data in Fig.6.2 show that the turbulent vertical flux has always opposite sign to the advective flux, although the magnitude is much smaller within the urban canopy (note that the scales of vertical fluxes are different for advective and turbulent cases). The turbulent transport reaches the same

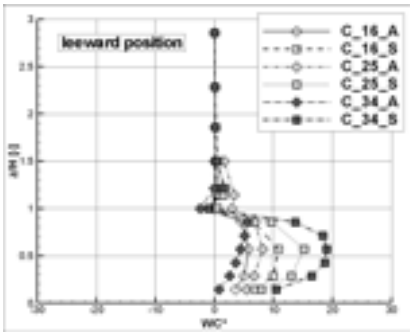

(a) Advection transport in leeward position.

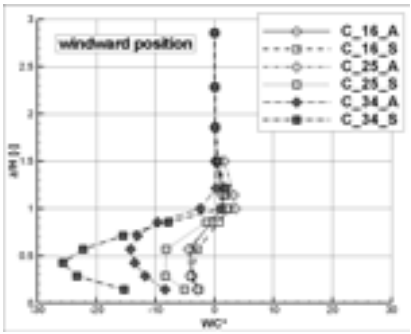

(b) Advection transport in windward position.

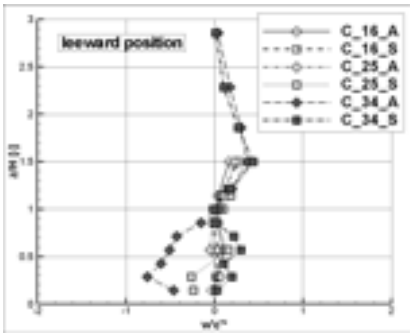

(c) Turbulent transport in leeward position.

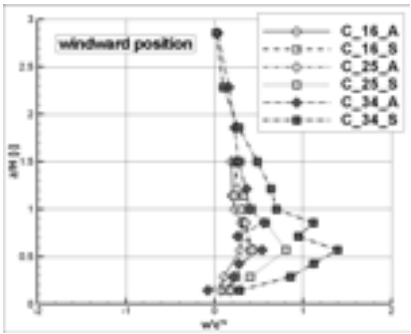

(d) Turbulent transport in windward position.

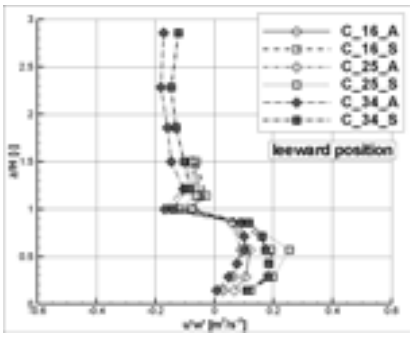

(e) Momentum transport in leeward position.

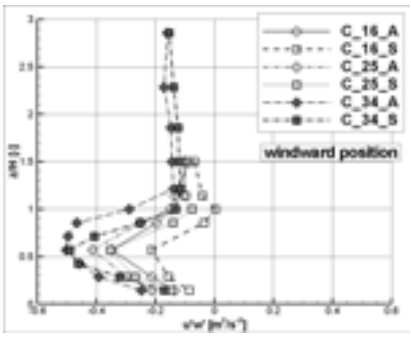

(f) Momentum transport in windward position.

FIG. 6.2. *Comparison of the normalised vertical turbulent, advective, and momentum transports in leeward and windward positions.*

magnitude as the advective flux at the roof top level and higher, where the mean value of vertical velocity and also the advective vertical flux become zero. The magnitude of both advective and turbulent transports is much higher in the case of staggered set-ups with higher packing densities (squares in darker colour in Fig.6.2). However, the influence of the packing density is less significant than the influence of the canopy arrangement. The highest values of both fluxes within the vertical profiles were found approximately in the middle of the obstacle height at all locations, followed by the rapid decrease in the case of advective flux. The turbulent fluxes showed significant values also above canopy, sometimes displayed secondary local maximum at height around 1.5H, and played significant role in the ventilation process of the passive contaminant.

The usual way of the parameterisation of the turbulent vertical fluxes is using the vertical profile of momentum transport, i.e. the Reynolds stress profile (Fig.6.2(e) and 6.2(f)). However, the measurements show that the Reynolds stress corresponds to advective fluxes and they should not be used for vertical turbulent transport parameterisation.

7. Conclusions. Pollutant dispersion within an urban canopy is very complicated process. We have chosen an idealised canopy created by regularly placed cubes to simplify the situation. The dispersion of the passive pollutant through an idealised urban canopy is greatly influenced by the initial spread from the source. This phenomenon is mainly driven by the layout of the obstacles, but not by packing density. The lateral spread of the pollutant just behind the source is higher for the aligned set-ups, while the pollutant is spreading laterally all the way downwind within the staggered arrangements. The plume shape is strongly dependent on the array layout. A diamond-shaped plume in the case of staggered set-ups occupies smaller area than a rectangle-shaped in the case of the aligned set-ups. This means that the ground level area threatened by the toxic gas release is larger due to weaker vertical transport in the less dense and aligned set-ups.

The comparison of the advective and turbulent fluxes within 6 different arrangements of idealised urban canopies has shown prevailing advective transport close to the building walls and significant contribution of the turbulent transport at the edge of the plume and at the roof top area. The strongest downward and upward advective transport of the passive contaminant was found at windward and leeward positions, respectively. This is in contrary to the findings inside the plant canopy, where the turbulent transport is important due to the porous nature of the plant canopy.

Urban canopy designers should consider the following suggestions to enhance the vertical transportation of passive contaminant. The urban canopies should be design to prevent aligned layouts, the more variable layouts will be applied the better. Urban canopy should be composed of lots of smaller structures build close to each other, i.e. with high packing densities, rather than large-blocks buildings.

Acknowledgment. This work was conducted by the financial support of the Japan Society for Promotion in Science. Authors also would like to thanks the project AV0Z20760514 of the Ministry of Education, Youth and Sports of the Czech Republic.

REFERENCES

[1] R. W. MacDonald, R. F. Griffiths, and S. C. Cheah, Field experiments of dispersion through regular arrays of cubic structures, *Atmospheric Environment, vol.31*, pp. 783-795 (1997)

[2] I. Mavroidis, Velocity and concentration measurements within arrays of obstacles, *Global Nest: the Int. J., vol.2*, pp.109-117 (2000)

[3] H. Cheng, P. Hayden, A. G. Robins, and I. P. Castro, Flow over cube array of different packing densities, *Journal of Wind Engineering and Industrial Aerodynamics, 95*, pp.715-740 (2007)

[4] D. J. Triton, *Physical Fluid Dynamics*, Oxford University Press (1988)

[5] J. E. Fackrell and A. G. Robins, Concentration fluctuations and fluxes in plumes from point sources in a turbulent boundary layer, *J. Fluid Mech., vol.117*, pp. 1-26 (1982)

[6] T. P. Meyers and D. D. Baldocchi, The budget of turbulent kinetic energy and Reynolds stress within and above a deciduous forest, *Agricultural and Forest Meteorology, vol.53*, pp. 207-222 (1991)

[7] R. Yoshie, H. Tanaka and T. Shirasawa, Technique for Simultaneously Measuring Fluctuating Velocity, Temperature and Concentration in Non-isothermal Flow, *Proceedings of the 12th International Conference on Wind Engineering, Cairns, Australia*, pp.1399-1406 (2007)

[8] R. B. Stull, *An Introduction to Boundary Layer Meteorology*, Kluwer Academic Publishers (1988)

[9] W. H. Snyder, Guideline for Fluid Modeling of Atmospheric Diffusion, *Report No. 600/8-81-009, Enviromental Sciences Research Laboratory, Office of Research and Development, U.S. Environmental Protection Agency, Research Triangle Park, NC 27711* (1981)

[10] J. C. Kaimal, J. C. Wyngaard, Y. Izumi, and O. R. Cote, Spectral characteristics of surface layer turbulence, *Quarterly Journal of the Royal Meteorological Society, 98*, pp.563-589 (1972)

[11] K. Bezpalcova, Newly implemented method for the boundary layer formation in a wind tunnel, *Wind Effects News, Vol. 17* (2007)

[12] T. R. Oke, *Boundary Layer Climates*, Routledge, London (1987)